Journal of Evolutionary Biology, 2024, **37**, 995–1008
https://doi.org/10.1093/jeb/voae083
Advance access publication 29 July 2024
Research Article

JOURNAL OF
Evolutionary Biology

eseb
European Society for Evolutionary Biology

Heterogeneous genomic architecture of skeletal armour traits in sticklebacks

Xueling Yi[1,4,*], Petri Kemppainen[1,2], Kerry Reid[1], Ying Chen[1], Pasi Rastas[3], Antoine Fraimout[2], Juha Merilä[1,2,*]

[1]Area of Ecology and Biodiversity, School of Biological Sciences, University of Hong Kong, Hong Kong, Hong Kong SAR
[2]Ecological Genetics Research Unit, Organismal and Evolutionary Biology Programme, University of Helsinki, Helsinki, Finland
[3]Institute of Biotechnology, HiLIFE, University of Helsinki, Helsinki, Finland
[4]Present address: Senckenberg Research Institute, Senckenberganlage 25, 60325, Frankfurt am Main, Germany.

Handling editor: Rebekah Rogers, Associate editor: Jun Kitano

Corresponding authors: Xueling Yi, Area of Ecology and Biodiversity, School of Biological Sciences, University of Hong Kong, Hong Kong, Hong Kong SAR. Email: xuelingyi5@gmail.com; Juha Merilä, Ecological Genetics Research Unit, Organismal and Evolutionary Biology Programme, University of Helsinki, Helsinki, Finland. Email: juha.merila@helsinki.fi
*Xueling Yi and Juha Merilä share the lead author position on this paper.

Abstract

Whether populations adapt to similar selection pressures using the same underlying genetic variants depends on population history and the distribution of standing genetic variation at the metapopulation level. Studies of sticklebacks provide a case in point: when colonizing and adapting to freshwater habitats, three-spined sticklebacks (*Gasterosteus aculeatus*) with high gene flow tend to fix the same adaptive alleles in the same major loci, whereas nine-spined sticklebacks (*Pungitius pungitius*) with limited gene flow tend to utilize a more heterogeneous set of loci. In accordance with this, we report results of quantitative trait locus (QTL) analyses using a backcross design showing that lateral plate number variation in the western European nine-spined sticklebacks mapped to 3 moderate-effect QTL, contrary to the major-effect QTL in three-spined sticklebacks and different from the 4 QTL previously identified in the eastern European nine-spined sticklebacks. Furthermore, several QTL were identified associated with variation in lateral plate size, and 3 moderate-effect QTL with body size. Together, these findings indicate more heterogenous and polygenic genetic underpinnings of skeletal armour variation in nine-spined than three-spined sticklebacks, indicating limited genetic parallelism underlying armour trait evolution in the family Gasterostidae.

Keywords: body size, lateral plate, parallel evolution, *Pungitius pungitius*, QTL

Introduction

Why and when evolution can be repeatable and predictable remains a longstanding question in biology. Parallel evolution has been the prevailing hypothesis explaining repeatable phenotypic evolution (Martin & Orgogozo, 2013) by the same set of genetic variants controlling the same adaptive traits in multiple independent evolutionary lineages (Schluter et al., 2004). The probability of parallel evolution depends on many factors (Bolnick et al., 2018; MacPherson & Nuismer, 2017), including how standing genetic variation is distributed at the metapopulation level (Fang et al., 2020, 2021; Kemppainen et al., 2021; Schlötterer, 2023). When populations are well connected, adaptive alleles are easily transported from one population to another and thereby available to be picked by selection in multiple populations subject to similar environmental pressures (Bailey et al., 2017; Lee & Coop, 2017; Ralph & Coop, 2015; Roberts Kingman et al., 2021). However, once gene flow is sufficiently restricted, the potentially adaptive alleles may not reach all populations, forcing selection to work with alternative alleles in different loci (Kemppainen et al., 2021; Merilä, 2014). The likelihood of parallel evolution is also influenced by demographic history of populations (MacPherson & Nuismer, 2017; Thompson et al., 2019): parallel evolution is less likely in small populations where bottlenecks and strong genetic drift result in the stochastic loss of adaptive alleles (Dahms et al., 2022; Fang et al., 2020; Leinonen et al., 2012). Accordingly, smaller and less connected populations tend to have more heterogeneous genetic architectures underlying the same morphological transitions even if driven by similar ecological pressures, resulting in non-parallel evolutionary responses to selection. Understanding the relative contributions of parallel and non-parallel genetic changes to repeated phenotypic evolution in the wild can improve theoretical understanding of the role of natural selection in shaping genetic variation (Johannesson, 2001) and inform predictions on the evolutionary potential of species and populations to cope with ongoing environmental changes (Bay et al., 2017).

While early research found ample evidence of genetic parallelism at both species and population levels (Bernatchez et al., 2010; Colosimo et al., 2005; Elmer et al., 2010; Stewart & Thompson, 2009), it is now becoming increasingly clear that parallelism is perhaps not as common as previously thought (e.g., Bolnick et al., 2018; Fang et al., 2020; Kemppainen et al., 2021; Schlötterer, 2023). The prevailing hypothesis of parallel evolution could thus stem from an ascertainment bias

Received February 1, 2024; revised April 28, 2024; accepted July 27, 2024

driven by the novelty value of discovering evidence for genetic parallelism, as well as from focusing on systems characterized by high genetic connectivity. On the other hand, non-parallelism is more likely to dominate in species characterized by low genetic connectivity and small effective population sizes. The stickleback fishes have been popular model systems to study the repeatability of evolution during their numerous and recurrent colonizations from marine to freshwater habitats throughout past glacial cycles (e.g., Chan et al., 2010; Colosimo et al., 2005; Coyle et al., 2007; DeFaveri et al., 2011, 2013; Fang et al., 2021; Jones et al., 2012; Kemppainen et al., 2021; Marchinko & Schluter, 2007; Merilä, 2013; Reid et al., 2021; Roberts Kingman et al., 2021). What has transpired from these studies is that in the case of the three-spined stickleback (*Gasterosteus aculeatus*), adaptation to the freshwater environment is often (but not always) achieved by parallel genetic changes in major-effect loci (Chan et al., 2010; Colosimo et al., 2005; Peichel & Marques, 2017; Reid et al., 2021); but see (DeFaveri et al., 2011; Erickson et al., 2016; Fang et al., 2021; Leinonen et al., 2012; Lucek et al., 2012; Poore et al., 2023; Yamasaki et al. 2019). However, in the case of the nine-spined stickleback (*Pungitius pungitius*), there is much less genetic parallelism over similar geographic distances in response to adaptation to freshwater environments (Fang et al., 2021; Kemppainen et al., 2021; Shikano et al., 2013). For example, pelvic reduction is underlain by one major-effect gene in different freshwater populations of three-spined sticklebacks (Chan et al., 2010; Xie et al. 2019), whereas in the case of nine-spined sticklebacks it is underlain by a range of genetic architectures from single locus to polygenic systems (Kemppainen et al., 2021).

A textbook example of predictable and repeatable evolution is the lateral plate reduction in freshwater three-spined sticklebacks after colonization from marine habitats, both in terms of plate number and plate size (Colosimo et al., 2005; Indjeian et al., 2016). The majority of their freshwater populations worldwide have achieved lateral plate reduction via inheritance of the same ancestral allele associated with the Ectodysplasin-A gene (*Eda*; Colosimo et al., 2005; O'Brown et al., 2015). This parallel evolution is attributed to both higher genetic connectivity among three-spined stickleback populations (Fang et al., 2021) and the large-effect single-locus basis for the adaptive reduction of lateral plates: quantitative trait locus (QTL) mapping studies have revealed that the QTL containing *Eda* gene explains 69%–98% variation in lateral plate phenotypes across different populations (Baird et al., 2008; Berner et al., 2014; Colosimo et al., 2004, 2005; Cresko et al., 2004; Erickson et al., 2016; Glazer et al., 2015; Liu et al., 2014; Schluter et al., 2021), although alternative small-effect QTL have also been identified (Colosimo et al., 2004; Conte et al., 2015; Erickson et al., 2016; Glazer et al., 2015; Laurentino et al., 2022; Liu et al., 2014; Loehr et al., 2012; Lucek et al., 2012; Poore et al., 2023; Yamasaki et al., 2019). However, in nine-spined sticklebacks, the *Eda* gene was not associated with lateral plate variation in populations from North America (Shapiro et al., 2009) or eastern Europe (Yang et al., 2016). Instead, the genetic architecture of lateral plate variation in the eastern European lineage (EL) of nine-spined sticklebacks was mapped to four different chromosomes (linkage groups LG8, LG12, LG20, LG21; Yang et al., 2016), none of which included the *Eda* gene. These studies thus suggest major interspecific differences in genetic architectures of lateral plate variation within the stickleback family Gasterosteidae, as well as a more polygenic and heterogeneous genetic architecture for this trait in the genus *Pungitius*.

This study aims to address the repeatable phenotypic evolution hypothesis (Martin & Orgogozo, 2013) in the context of genetic architectures of lateral plate phenotypes in *Pungitius* sticklebacks. To test the hypothesis of parallel evolution, we mapped QTL associated with variation in lateral plate numbers and sizes (*viz*. area, width, height) utilizing a backcross family between two closely related *Pungitius* species: the fully plated *P. sinensis* population from Odate, Japan (Takahashi et al., 2001), and the partially plated *P. pungitius* population from the western European lineage (WL; average 5.4 and range 3–11 lateral plates; Banarescu & Paepke, 2001). The reduction of plate number is expected to accompany a reduction of plate size, as observed in the freshwater three-spined sticklebacks (Berner et al., 2014; Colosimo et al., 2004; Indjcian et al., 2016). The WL *P. pungitius* has a distinct evolutionary history from the eastern EL (Feng et al., 2022; Guo et al., 2019; Teacher et al., 2011) and has not yet been studied regarding their armour plate genetic architecture. The repeatable evolution hypothesis predicts that lateral plate variation in the WL should be controlled by allelic variation either in the same genetic locus as that in the sister species three-spined stickleback or the previously identified QTL in the EL *P. pungitius*. The alternative hypothesis of non-parallel evolution of the same morphology underlain by different QTL is also plausible in the light of previous QTL analyses of lateral plate number variation in *Pungitius* sticklebacks (Shapiro et al., 2009; Yang et al., 2016). We also identified QTL associated with body size variation and phenotypic sex using this cross.

Material and methods

Crosses and fish rearing

A fully plated female *P. sinensis* from Yoneshiro River, Odate, Japan (40°16′ N, 140°29′ E) was artificially crossed with a partially plated male *P. pungitius* from Brugse polders, Maldegem, Belgium (51°10′ N, 03°28′ E). The *P. pungitius* population from Belgium is a genetically isolated freshwater population (Feng et al., 2022). The *P. sinensis* population from Yoneshiro River may be connected with marine populations but genetic divergence (Wang et al., 2015) indicated a low degree of connectivity between this population and other *P. sinensis* populations. The F_1 hybrids were reared in a 28-L tank at 16 °C until mature. The F_1 hybrid males of these crosses were found to be sterile (Natri et al., 2019), and thus a backcross was conducted by naturally mating a partially plated F_1 hybrid female with an outbred fully plated *P. sinensis* male (Figure 1). This backcross mating was carried out in a 6-L tank with a zebrafish rack system (Aquaneering Inc., USA) to obtain fertilized clutches repeatedly. From 3 days post-hatching, larvae were fed twice daily with newly hatched brine shrimp (*Artemia sp*.) nauplii. Approximately 8 weeks post-hatching, frozen bloodworms (Chironomidae larvae) were added to their diet. The 24-hr photoperiod was maintained during the rearing. Wild fish were obtained in accordance with national and institutional ethical regulations with permission from the Finnish Food Safety Authority (#1181/0527/2011 and #3701/0460/2011). All fish rearing was conducted under the license from the Finnish National Animal Experiment Board (#STH379A and #PH1236A).

The F_2 progeny were reared in 28-L tanks (20–30 fish per tank) at 16 °C for 40 weeks after hatching. At the end

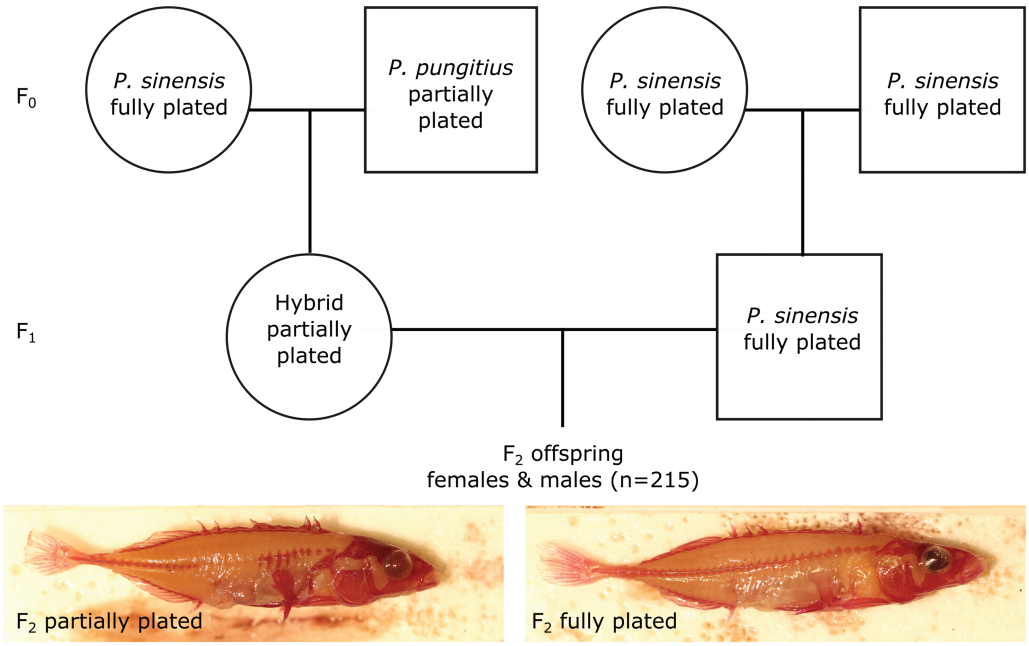

Figure 1. The backcross experiment between fully plated *Pungitius sinensis* from Japan and partially plated *P. pungitius* from Belgium. Circles represent females and squares represent males. The two photos show fully plated and partially plated phenotypes of the stained F_2 progeny.

of the experiments, the wild-caught grandparents (F_0), F_1 parents, and F_2 offspring were euthanized with MS-222 (Tricaine methanesulfonate) and stored in ethanol. A fin clip was taken from all individuals and preserved at −18 °C for DNA extractions. In total, 215 F_2 offspring from six clutches were available for the analyses (Supplementary Table S1). Phenotypic measurements (see below) were taken from these F_2 offspring and their sex was recorded based on gonadal inspection after dissection.

Phenotypic measurements

Firstly, the ethanol-stored carcases of F_2 offspring were fixed in 4% formalin and stained with alizarin red following the standard procedure (e.g., Trokovic et al., 2011) to visualize bony structures. Subsequently, phenotypes were quantified by ImageJ (https://imagej.nih.gov/ij/index.html) from photographs (Figure 1; Supplementary Figure S1) of the stained fish. Standard length (SL) and maximum body height (BH) of each specimen was measured to nearest 0.01 mm from the photographs.

Plate and myomere (blocks of skeletal muscle tissue arranged in sequence) numbers were counted on both sides of the body under a dissecting microscope. The proportion of plated myomeres on each side was calculated to represent the level of plateness. The height, width, and surface area of the largest lateral plates were measured on both sides of the body. Most of the largest plates were found on myomere seven counted from the anterior part of the body towards the tail (Supplementary Figure S1). If the fish had no plate in these positions, the largest plate located within the first 15 anterior myomeres were measured instead with their myomere position recorded. We did not measure plates on the myomere positions > 15 because plates in the posterior region have distinct shapes and sizes compared to those in more anterior positions. Measurements of the same phenotype on the left and right sides of the body were highly correlated ($r > 0.86$, $p <$ 1e-10; Supplementary Figure S2). Therefore, in the following analyses we used average values of each measurement of the two sides.

The distribution of phenotypic measurements was visualized in R (R Core Team, 2022). Traits fitting the normal distribution (namely SL, BH, plate area, plate height, and plate width; Supplementary Figure S3) were analysed using raw values. Distributions of the plate number and the proportion of plated myomeres were left-skewed and bimodal because of the presence of only fully- and partially plated individuals (Supplementary Figure S3). This pattern is related to our experimental design (Figure 1) where offspring genotypes can only be *P. sinensis* homozygotes (SS, likely fully plated) or *P. sinenesis-P. pungitius* heterozygotes (SP, likely partially plated). Therefore, the missing *P. pungitius* homozygous genotypes likely account for the lack of low-plated individuals and the left skew of plate number distribution. The plate number was analysed as either a numeric trait (the mean number of plates, plateN_mean) or a binary trait using two different transformations. First, the plate number was transformed into a binary trait, plateN_binary, where individuals were labeled as partially plated if having the mean number of plates ≤ 25 (around the peak of the first phenotype cluster, Supplementary Figure S3) and the rest of the individuals were fully plated. Second, the proportion of plated myomeres was transformed into the binary trait, plateness, where individuals having 100% plated myomeres on both sides were considered fully plated while the rest were partially plated.

Sequencing and genotyping

DNA was extracted from the preserved fin-clips of wild-caught grandparents, F_1 hybrid parents, and F_2 offspring using the modified salting out method (Sunnucks & Hales, 1996). Libraries for the restriction-site associated DNA sequencing (RADseq) were prepared using the *PstI* restriction enzyme (Miller et al., 2007). The prepared libraries were sequenced on an Illumina HiSeqTM 2000 (BGI Hong Kong). Demultiplexed raw sequencing data were obtained from BGI

with adapter and low-quality reads removed. These reads were around 43 bp in length and they were mapped to the reference genome of *Pungitius pungitius* (version 7, GenBank GCA_902500615.3; Kivikoski et al., 2021) using the BWA v0.7.17 backtrack algorithm (bwa aln and bwa samse; Li & Durbin, 2009). The mapped reads were reformatted, sorted, and indexed using SAMtools version 1.16.1 (Danecek et al., 2021). Genotyping was conducted according to the sequencing data processing pipeline of Lep-MAP3 (Rastas, 2017). Briefly, SAMtools mpileup (Li, 2011) was run on the mapped data by linkage group. The version 7 reference genome has 21 linkage groups (LGs) and 1,645 unassembled contigs (including a mitochondrial genome). Very few data were mapped to the unassembled contigs whose physical positions were unclear. Therefore, we only used the data mapped to the 21 LGs as the input of the Lep-MAP3 module Pileup2Likelihoods to estimate genotypes.

Linkage map construction

Linkage maps were constructed following the Lep-MAP3 default pipeline (Rastas, 2017). Briefly, the module ParentCall2 was run on all genotyped individuals (offspring, parents, grandparents) with the noninformative sites removed (removeNonInformative = 1). The retained genotypes were processed by the module Filtering2 with the parameter dataTolerance = 0.001 (i.e., segregation distortion limit 1:1,000). Then the module SeparateChromosomes2 was run to assign markers to LGs (ordered by size) using the parameter lodLimit = 50. The first (i.e., largest) 21 LGs were retained, corresponding to the number of chromosomes in the reference genome (Supplementary Figure S4). The linkage map was modified by collapsing all the other LGs with unassigned singletons. Next, the module JoinSingles2All was run using the modified linkage map and the non-filtered genotyping data (the output from ParentCall2) to map as many singletons to the 21 LGs as possible, using the parameters lodLimit = 40, lodDifference = 2, lod3, Mode = 3, iterate = 1, and distortionLod = 1. Finally, the module OrderMarkers2 was used to order markers in the mapped 21 LGs and generate phased maternal maps using commands outputPhasedData = 1 and informativeMask = 2.

To get optimal results, OrderMarkers2 was run five times independently for each linkage group and the runs having the highest likelihoods were used as the optimal parent-phased maps. These optimal maps were then evaluated in OrderMarkers2 (command evaluateOrder) with additional parameters improveOrder = 0 and grandparentPhase = 1 to convert them into grandparental phases. The optimal parental phases and corresponding grandparental phases were matched using the phasematch.awk script of Lep-MAP3. The matched maps were converted back to genomic coordinates using the awk script in Lep-MAP3, and the maps were re-named by chromosomes based on the physical positions of their markers. In each map, the few markers that were located in different physical chromosomes were removed. Then the converted linkage maps were visualized by plotting the genetic position (centiMorgan, cM) against the physical position (bp), and the maps were further cleaned by manually removing the outlier markers and markers that generated gaps at the start or end of each linkage map. Finally, the map2genotypes.awk script of Lep-MAP3 was used to convert the cleaned maps into F_2 genotypes.

QTL mapping

The QTL mapping was conducted using the software R/qtl2 (Broman et al., 2019). The genotypes and linkage maps obtained from Lep-MAP3 were reformatted for R/qtl2 using custom scripts. Backcross (bc) cross type was specified in the control files. Pseudomarkers were inserted into genetic maps at the distance of 1 cM. Genotype probabilities were calculated using the error probability of 0.002. Genotype-phenotype associations were estimated by conducting genome scans (command scan1) using the default simple linear method of the Haley–Knott regression for the numeric traits and the binary model for the binary traits. The other R/qtl2 parameters were kept as default unless stated otherwise. Statistical significance thresholds were established using 1,000 permutations (command scan1perm). The obtained significance threshold ($p = 0.05$) was used to identify QTL peaks and their 95% Bayes credible intervals using the command find_peaks (peakdrop = 2).

We first conducted QTL mapping on the binary phenotypic sex and identified genetic sexes (see Supplementary materials). Preliminary analyses on all 215 F_2 offspring indicated mismatched genetic and phenotypic sexes in 11 individuals which were removed together with the phenotypic sex-unknown individual (Supplementary Table S1) from downstream analyses for clarity.

QTL mapping on the body size measurements (SL and BH) was carried out with sex and clutch included as additive covariates (argument addcovar) because both phenotypes showed significant dependency on sex and clutch in tests of the Analysis of Variance (ANOVA; Supplementary Table S2). For the binary traits (plateN_binary and plateness), we tested their dependency on sex and clutch identities using the Pearson's Chi-squared test and their dependency on the SL and BH using *t*-tests. None of the variables showed significant relationships ($p > 0.05$) with either binary traits. Therefore, no covariate was added in the QTL mapping of plateN_binary or plateness. For each of the other numeric traits (plate number, plate area, plate height, plate width), the dependency on sex and clutch was first tested using ANOVA. Then a generalized linear model of each trait was fitted on the detected significant independent variables, and the residuals were used to further test dependency on SL and BH (i.e., with sex and clutch controlled; Miller et al., 2014). All significant independent variables were then included as additive covariates in the QTL mapping of the corresponding trait (Supplementary Table S2).

The genomic regions spanning the 95% CIs around significant QTL were considered as QTL regions. The percentage of phenotypic variation explained (PVE) by each significant QTL peak was calculated as $PVE = 1 - 10^{-\frac{2}{n}*LOD}$, where n is the sample size and LOD is the logarithm of the odds of the QTL peak (Broman & Sen, 2009; Smith et al., 2020). In addition, for each trait, we also used a previously described lasso regression approach to jointly incorporate all SNPs into a multilocus model to estimate the total PVE value that approximates the narrow sense heritability of a given trait (Kemppainen et al., 2021; Li et al., 2017, 2018). To facilitate calculation of the lasso algorithm, the same genotype file as used for R/qtl2 analyses was re-coded by removing duplicate SNPs that had the same genotypes (2,677 SNPs retained) and merging all SNPs outside significant QTL regions into one chromosome representing the non-QTL region. For each trait

Table 1. The QTL peaks for phenotypic traits.

Phenotype	LG	Peak (cM)	95%CI low (cM)	95%CI high (cM)	Range (cM)	LOD	PVE (%)	NO. SNPs in 95% CI
Sex	12	11.286	10.819	11.286	0.467	61.08	74.98	18
Sex	12	13.623	13.623	14.090	0.467	51.25	68.74	25
Standard length	12	87.896[a]	81.591	92.927	11.336	5.35	11.43	139
Standard length	16	43.088	32.301	45.438	13.137	7.21	15.08	110
Body height	6	55.305	42.172	63.721	21.549	4.98	10.68	547
Plate number	4	137.699	133.021	137.699	4.678	4.58	9.87	1,531
Plate number	13	64.174	60.436	65.109	4.673	9.09	18.64	428
Plate number	17	62.363	47.838	70.352	22.514	5.16	11.04	2,677
Plateness	13	63.240	56.693	65.109	8.416	4.92	10.57	494
Plate area	19	36.939[b]	30.427	58.042	27.615	3.68	8.01	2,512
Plate area	20	53.440	48.767	53.440	4.673	9.63	19.63	1,642
Plate height	20	53.440	49.234	53.440	4.206	13.02	25.58	1,626
Plate width	17	65.635	48.772	70.352	21.580	3.84	8.33	2,663
Plate width	19	33.707	4.677	56.172	51.495	3.26	7.12	2,688
Plate width	20	53.440	50.169	53.440	3.271	5.81	12.35	1,597

Note. LG = linkage group; cM = centimorgan; PVE = percentage of variation explained.
[a]Pseudomarker (the nearest non-pseudo genetic position at 88.191).
[b]Pseudomarker (the nearest non-pseudo genetic position at 36.043).

(excluding sex), the total PVE was estimated using all remaining SNPs, and the PVE of each QTL was estimated using the SNPs corresponding to the given QTL region. All phenotypic analyses and QTL mapping were conducted using R version 4 (R Core Team, 2022).

QTL effects and candidate genes

As we were mostly interested in traits related to lateral plate variation (i.e., plate number and plate size), we further estimated the effects of all the combinations of identified QTL peaks in these traits. QTL effects were estimated using the command scan1coef and plotted using plot_coef in R/qtl2. The most likely genotypes of the analysed F_2 offspring at each QTL peak were extracted using the command maxmarg in R/qtl2. Phenotypes were plotted against genotypes at each QTL peak position and by combinations of all identified QTL peaks.

For each QTL region, we extracted all physical markers which mapped to genetic positions within these regions and identified all genes containing these physical markers. Gene lists were made using the annotation of the version 6 reference genome (Varadharajan et al., 2019) and liftover between version 6 and version 7 reference genomes (Rastas, 2020; https://sourceforge.net/p/lep-anchor/code/ci/master/tree/liftover.awk).

Results

Genotyping and linkage maps

The final dataset consisted of 221 individuals which included four F_0 grandparents, two F_1 parents, and 215 F_2 offspring (Figure 1). The Lep-MAP3 Pileup2Likelihoods module identified 170,339 SNPs across the 21 LGs of which 84,526 informative sites were retained by ParentCall2. The largest 21 LGs identified by SeparateChromosomes2 contained 61,863 markers (Supplementary Figure S4) and the remaining 22,663 sites were designated as singletons. Finally, JoinSingles2All further added 7,485 sites into the LGs, resulting in a total of 69,348 sites separated into 21 LGs. Preliminary results showed that fewer than 8% of markers were paternally informative (i.e., using informativeMask = 13) while more than 92% of the markers were maternally informative (informativeMask = 23). This observation may not be surprising given that only the F_1 mother was hybrid and that the males in general have fewer crossovers (Kivikoski et al., 2023). In addition, the *P. pungitius* reference genome was used which was more similar to the hybrid F_1 female than the F_1 male (*P. sinensis*). Therefore, only the maternally informative markers were utilized in the following analyses. The phased and matched maternal maps had a total of 60,089 sites, and 59,629 sites were retained after the manual cleaning (Supplementary Figure S5).

Among the 215 F_2 offspring, 203 individuals showed consistent genetic and phenotypic sexes (Supplementary material) and were retained in the QTL analyses. The phenotypic sex was mapped to two LG12 QTL (in total 1 cM) with non-overlapping 95% CIs (Table 1) and contained 43 SNPs located within six genes (*Usp7*, *EFS*, *DHRS4*, *Slc7a8*, *Svep1*, and *TBC1D19*; Supplementary Table S3).

QTL mapping of lateral plate phenotypes

Most of the lateral plate phenotypes were significantly dependent on phenotypic sex (Supplementary Table S2). Females had more (x = 30.1 ± 0.45 [S.E.]) and bigger (x = 2.0 ± 0.10 mm^2) lateral plates than males (plate number: x = 28.7 ± 0.52, plate area: x = 1.6 ± 0.08 mm^2). However, this sexual dimorphism is confounded by body size (females are larger, see below), as t-tests of plate number and plate size between sexes were not significant ($p > 0.05$) after controlling for SL (i.e., when using the residuals of linear regressions against SL). Both plate number and the percentage of plated myomeres (*viz.* plateN_mean, plateness) were associated with a QTL at almost the same peak position in LG13 with overlapping confidence intervals (Table 1; Supplementary Figure 2A). In addition, plate number was associated with QTL on LG17 and LG4 (Supplementary Figure 2A), the latter containing the candidate gene *Eda* that controls lateral plate phenotypes in three-spined sticklebacks (Colosimo et al., 2004). Almost identical QTL regions were found when using the raw values of the plate number (plateN_mean; Table 1) and the transformed binary trait (plateN_binary; Supplementary Table S4; Supplementary Figure S6), providing confidence of the identified regions being true QTL rather than false positives despite a skewed distribution of raw plate numbers. Both the LG4 and the LG13 QTL showed a positive effect of the *P. sinensis*—*P. pungitius* hybrid genotype (SP) whereas the LG17 QTL showed a negative effect of the SP genotype on lateral plate numbers (Figure 3A). Consistently, among the eight genotype combinations of these three QTL, the genotype having SS at both LG4 and LG13 but SP at LG17 generated the lowest number of lateral plates, while the reverse (SP at LG4 and LG13 while SS at LG17) generated the highest number of lateral plates (Figure 3B).

The lasso regression approach produced a genomic estimate of heritability (h^2) at 0.486 (Supplementary Table S5), a value higher than the summed PVEs of the three plate number QTL (Sum_{PVE} = 0.396; Table 1), indicating that there might be additional QTL influencing plate number, albeit their contributions are likely to be minor.

The plate size phenotypes (*viz.* area, height, and width of the largest plate) were all associated with the same QTL peak on LG20 (Table 1; Figure 2B). Plate area and plate width also mapped to nearby QTL peaks on LG19, but their 95% CIs were almost as wide as the entire LG including large regions of LOD scores below the significance threshold (Supplementary Figure S7). In addition, plate width also mapped to LG17, overlapping with the QTL for plate number (Table 1). All SP genotypes at these QTL peaks had positive effects except for the LG17 QTL in which SP had a negative effect on plate width (Supplementary Figure S8), similar to its negative effect on plate number (Figure 3). Therefore, SP genotype at both LG19 and LG20 QTL peaks yielded the largest plate size and SP genotype at LG20 yielded the largest plate height, whereas SP genotype at both LG19 and LG20 and SS genotype at LG17 yielded the largest plate width (Supplementary Figure S9).

The lasso regression approach produced genomic heritabilities higher than the summed PVEs in plate area (h^2 = 0.495; Sum_{PVE} = 0.276), plate height (h^2 = 0.501; Sum_{PVE} = 0.256), and plate width (h^2 = 0.317; Sum_{PVE} = 0.278; Table 1, Supplementary Table S5), suggesting that additional unidentified loci may influence variation in these traits.

QTL mapping of body size

Females were significantly larger than males both in terms of SL ($x_{females}$ = 52.9 ± 0.57 [S.E.] mm; x_{males} = 49.0 ± 0.44 mm;

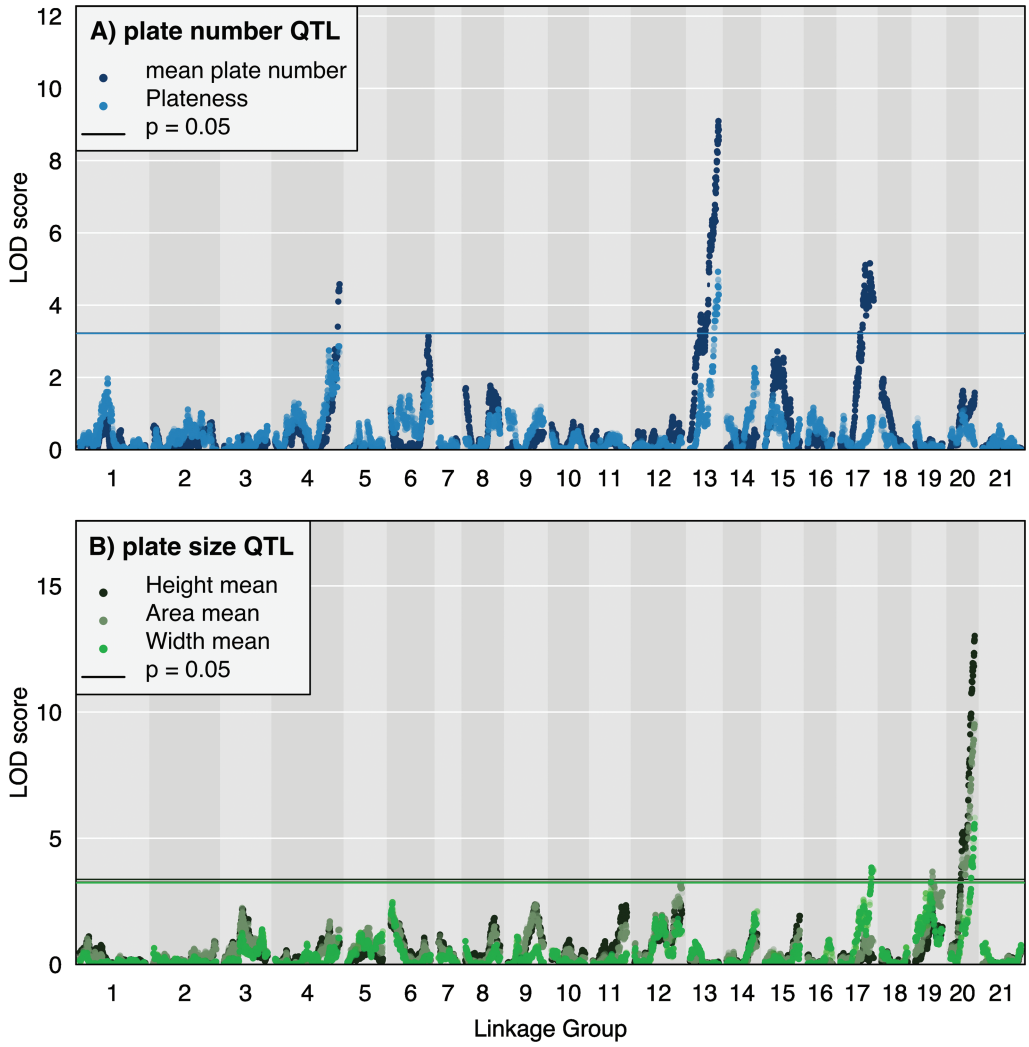

Figure 2. The QTL for lateral plate (A) number and (B) size in nine-spined sticklebacks. Horizontal lines show the significance threshold ($p = 0.05$) derived from 1,000 permutation tests for each trait.

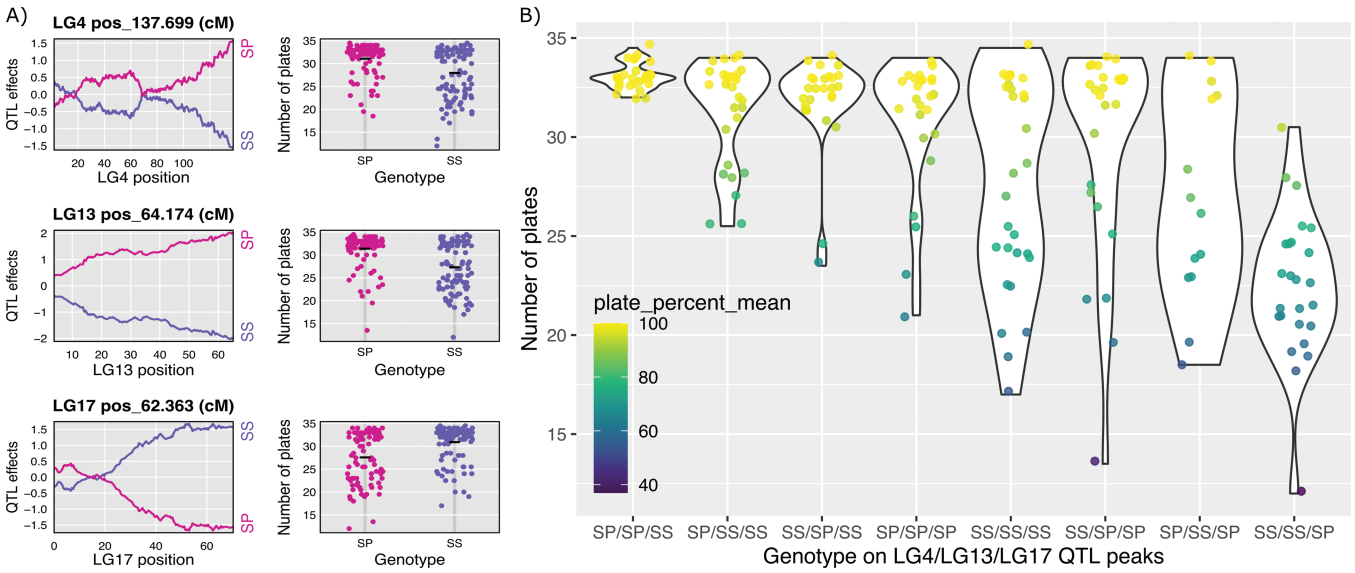

Figure 3. Effects of the genotypes at QTL peaks on lateral plate numbers. S represents the paternal allele from *P. sinensis* and P represents the maternal allele from *P. pungitius*. (A) Genotype effects of each QTL peak for the plate number variation, estimated by R/qtl2. (B) Distribution of individual number of plates by genotype combinations at the three QTL. The colour gradient indicates the per-individual percentage of plated myomeres (average of left and right body sides).

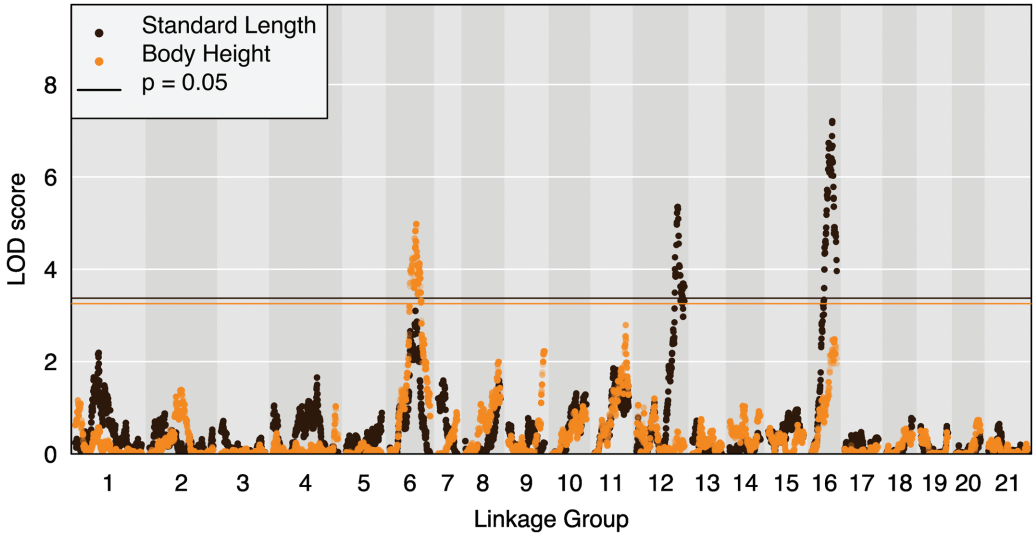

Figure 4. The QTL regions of body size variation. Horizontal lines show the significance threshold ($p = 0.05$) derived from 1,000 permutation tests for each trait.

$t_{190.36} = 5.33$, $p < 0.05$) and BH ($x_{females} = 11.0 \pm 0.15$ mm; $x_{males} = 10.4 \pm 0.09$ mm; $t_{174.57} = 3.28$, $p < 0.05$). Two moderate-effect QTL at LG12 and LG16 influenced SL and a QTL on LG6 influenced BH (Table 1; Figure 4) with sex as a covariate. Notably, the LG12 QTL for SL (81.59–92.93 cM) is located in a different region far away from the LG12 QTL for sex (13.62–14.09 cM), supporting this loci as a true QTL associated with SL rather than being confounded by sex. The lasso method estimated genomic heritabilities of $h^2 = 0.263$ for SL and $h^2 = 0.206$ for BH (Supplementary Table S5), and the corresponding summed PVEs across QTL were $Sum_{PVE} = 0.265$ for SL and $Sum_{PVE} = 0.107$ for BH (Table 1). It is noteworthy that the peak on LG6 in the analysis of SL was close to significance (Figure 4), indicating that this region might also affect SL by affecting the BH.

Candidate genes

All genes containing SNPs in identified QTL regions are listed in Supplementary Table S3. For the plate number variation, we identified several candidate genes whose functions might be associated with stickleback skeletal development, including the *Eda* gene on LG4, the fibroblast growth factors on LG4 (*Fgf4*, *Fgf16*, *Fgf20*; Jovelin et al., 2007), the bone morphogenetic protein genes on LG17 (*Bmp7*, Shawi & Serluca, 2008; *Bmp11*, Indjeian et al., 2016), and potentially the BMP-2-inducible protein kinase on LG13 (*Bmp2k*, Wang et al., 2020; X. Li & Cao, 2006). For the plate size variation, the *fgf23* on LG19 and the *Bmp7* and *Bmp11* on LG17 were identified as candidate genes. The BMP family in particular has been suggested to control the height and width of armour plates in sticklebacks (Indjeian et al., 2016). In addition, the paired box proteins (*Pax6* on LG19 and *Pax7* on LG17) have been found associated with the development of vertebrae in lab mice (Lang et al., 2007) and thus might also be candidate genes controlling the armour plate development in sticklebacks. The *Fgf14* on LG16 was identified as a candidate gene controlling the body size development.

Discussion

Our study shows that variation in lateral plate number and plate size in the WL of nine-spined sticklebacks is polygenic, controlled by several small- to medium-effect QTL on different chromosomes. Most of the identified QTL peaks are different from those found in previous studies of lateral plate variation in the eastern EL of nine-spined sticklebacks or in three-spined sticklebacks (Table 2). Although independent QTL studies are not directly comparable due to differences in parental populations and rearing environments, the overall trend holds true that early QTL studies of three-spined sticklebacks mostly find the same major-effect locus (i.e., the *Eda* gene) for lateral plate variation, whereas QTL studies of nine-spined sticklebacks tend to find more variable genetic regions of small to medium effects (Table 2). These results are consistent with the observation that pelvic armour morphology in nine-spined sticklebacks is also more polygenic and heterogeneous (Kemppainen et al., 2021), whereas pelvic reduction in three-spined sticklebacks is controlled by one major-effect gene *pitx1* although via different mutations across populations (Xie et al. 2019). Albeit several studies, typically from landlocked freshwater populations with limited gene flow, have also indicated less parallel evolution in different three-spined stickleback populations (Erickson et al., 2016; Fang et al., 2020; Lucek et al., 2012; Poore et al., 2023; Yamasaki et al., 2019). Hence, this study comprises yet another example of similar phenotypic changes likely being achieved by a variety of genetic architectures ranging from monogenic to oligo- or polygenic systems in the stickleback family Gasterosteidae (Colosimo et al., 2005; Kemppainen et al., 2021; Shapiro et al., 2009; Yang et al., 2016), rather than due to genetic parallelism governed by a few large-effect loci. Our findings highlight the notion that a diversity of genetic architectures can evolve to underpin similar phenotypic transitions, and that the frequency of reuse of the same genetic variation to achieve a given phenotypic transition (i.e., parallel evolution) differs between three- and nine-spined sticklebacks. Therefore, although freshwater populations of nine-spined sticklebacks are characterized by both small effective population sizes and low genetic connectivity (Fang et al., 2021; Kivikoski et al., 2023; Merilä, 2014; Shikano et al., 2010), our results together with recent studies (Kemppainen et al., 2021; Yang et al., 2016) highlight that these two population demographic parameters alone do not necessarily limit

Table 2. Comparison of the genetic architecture underlying the variation of lateral plate number and size in stickleback fishes.

Species	Lateral plate number		Lateral plate size		Reference
	QTL	PVE (%)	QTL	PVE (%)	
Gasterosteus aculeatus (Canada)	LG13	8.5	–	–	Peichel et al. (2001)
	LG26[a]	10			
Gasterosteus aculeatus (Japan × Canada)	LG4	76.9	LG4	11.5–12.9	Colosimo et al. (2004); finer mapping on LG4 in Colosimo et al. (2005)
	LG7	3.7	LG7	10.3–11.1	
	LG10	6.5	LG25[a]	17.9–28.9	
	LG26[a]	4.5			
Gasterosteus aculeatus (Alaska)	LG18	–	–	–	Cresko et al. (2004)
Gasterosteus aculeatus (Alaska)	LG4	–	–	–	Baird et al. (2008)
Gasterosteus aculeatus (Central Europe)	LG4	76	LG4	5.5–11.8	Berner et al. (2014)
			LG9	7.7	
			LG11	8.4–12.7	
Gasterosteus aculeatus (Canada)	LG2	0.22–4.9	–	–	Conte et al. (2015)
	LG7	0.47–12.09			
	LG16	0.31–6.06			
Gasterosteus aculeatus (Finland)	LG4	74.4	–	–	Liu et al. (2014)
	LG9	9.1			
	LG21	10.6			
Gasterosteus aculeatus (Canada × US)	LG4	95.7–97.8	–	–	Glazer et al. (2015)
	LG7	13.3[b]			
Gasterosteus aculeatus (Canada)	LG1	1.5–1.6	–	–	Erickson et al. (2016)
	LG3	2.4			
	LG4	68.8–75.8			
	LG5	4.5			
	LG7	2.9–4.2			
	LG21	1.6–7.5			
Gasterosteus aculeatus (Japan × Canada)	–	–	LG20	9.9-19.3	Indjeian et al. (2016)
Gasterosteus aculeatus (Canada)	LG4	85.8	–	–	Schluter et al. (2021)
Gasterosteus aculeatus (Canada)	LG2	–	–	–	Poore et al. (2023)
	LG4				
	LG7				
	LG16				
	LG17				
Pungitius pungitius (Canada × Alaska)	LG12[c]	28.4–30.1	–	–	Shapiro et al. (2009)
Pungitius pungitius (Finland EL)	LG8	8.7	–	–	Yang et al. (2016)
	LG12	7.3			
	LG20	8.0–11.3			
	LG21	8.6–10.0			
Pungitius pungitius	LG4	9.9	LG17	8.3	This study
(Japan *P. sinensis* × Belgium WL)	LG13	18.6	LG19	7.1–8.0	
	LG17	11	LG20	12.4–25.6	

Note. Populations used in the cross experiments are given in parentheses. The summary of QTL associated with plate size includes analyses of plate area, height, and width. EL = eastern European lineage; WL = western European lineage.
[a]The original linkage group studies in *Gasterosteus aculeatus* were based on a linkage map with 26 linkage groups before consolidation to the 21 confirmed chromosomes.
[b]Residual variance in *Eda* heterozygotes.
[c]The same region control sex.

evolutionary potential but rather result in a higher diversity of alleles underlying adaptive evolution.

Our results indicate that the genetic basis of lateral plate variation in the WL nine-spined sticklebacks is controlled by several distinct moderate-effect QTL on different LGs, as well as unknown small-effect loci potentially across the genome as revealed by the lasso analyses. One of the moderate-effect QTL on LG4 contained the *Eda* gene known to be the

major-effect locus typically explaining ~69%–98% variation in lateral plate numbers in three-spined sticklebacks (Table 2; Baird et al., 2008; Berner et al., 2014; Colosimo et al., 2004, 2005; Cresko et al., 2004; Erickson et al., 2016; Glazer et al., 2015; Liu et al., 2014; Schluter et al., 2021). However, this moderate-effect QTL explained only ~9.9% of variation in lateral plate numbers in WL nine-spined sticklebacks. The two other QTL associated with lateral plate number variation in our study were located on LG13 and LG17 and they accounted for 18.6% and 11.0% of variation, respectively. Hence, collectively the three QTL identified in this study accounted for up to 39.6% of variation in lateral plate numbers. Similarly, three QTL regions on LG17, LG19, and LG20 were associated with the lateral plate size in WL nine-spined sticklebacks and accounted for up to 28% of variation. It should be noted that potential low-plate recessive homozygotes (PP) are missing in our backcross design, which would have limited our power in detecting such QTL loci. The estimation of QTL effect sizes may be also influenced by sample size (the Beavis effect), recombination rate, mutation rate, gene density, and pleiotropy (Liu et al., 2014; Rennison & Peichel 2022; Roesti 2018). However, the previous study using intercrosses of EL nine-spined sticklebacks also found a similar amount of variation (33%) in plate numbers explained by four small- to medium-effect QTL (Yang et al., 2016). Therefore, despite potential caveats from the (modified) backcross design, our QTL results most likely reflect the true biological feature of nine-spined sticklebacks which has a more heterogeneous architecture (i.e., involving multiple moderate-effect genetic loci) of armour trait variation compared to most three-spined stickleback populations. Because large-effect sizes are more likely to be significant and detected as QTL regions, genetic loci of small-effect sizes may not be detected due to lack of statistical power. In accordance with this, estimates from lasso regressions suggested undetected small-effect loci (among the non-QTL SNPs) accounting for the unexplained variation (14% in mean plate number, 37% in plate area, 34% in plate height, and 20% in plate width, Supplementary Table S5), indicating oligo- to polygenic inheritance of these traits. These results are thus consistent with previous findings that genetic architectures of pelvic reduction in nine-spined sticklebacks range from monogenic to oligogenic and polygenic inheritance (Kemppainen et al., 2021). Although the QTL effect size may not be correlated with the QTL reuse (Conte et al., 2015), none of the QTL controlling lateral plate numbers are shared between EL and WL fishes. Therefore, the genetic architecture of lateral plate numbers appears to be divergent not only between the genera *Gastoresteous* and *Pungitius* but likely also within the genus *Pungitius*.

A few plate-associated QTL showed positive effects of the SP genotype compared to the SS genotype, indicating that the P allele at those loci could increase the plate number or size even at the presence of the S allele which is inherited from the completely plated *P. sinensis*, which is opposite of the expectation. A potential explanation is that the P allele at these loci might contribute to the maintenance of the partial lateral plates in this freshwater population of *P. pungitius* under balancing selection or due to genetic drift. In addition, it has been found that pleiotropy often involves antagonistic effects that would result in the opposite direction of QTL effects (Albert et al., 2008). However, the indicated P allele effects should be interpreted with caution because PP homozygotes are lacking in our backcross data. In addition, we observed plate number variation in the F_2 offspring that carry the parental *P. sinensis* genotype (i.e., SS/SS/SS, Figure 3B), which indicates additional effects from genomic regions outside the detected QTL, consistent with the genomic estimates of heritability suggesting presence of undetected QTL.

Among the moderate-effect QTL (on LG6, LG12, and LG16) explaining variation in SL and BH of the WL nine-spined sticklebacks, only the LG12 QTL is shared with the QTL affecting body size in the EL nine-spined sticklebacks (on LG8, LG12, and LG13; Laine et al., 2013). Therefore, the body size variation also appears to have different genetic architectures between EL and WL fishes, but different study designs (backcross vs. intercross) and parental populations (WL vs. EL) might have contributed to the difference between QTL results. In addition, it is unclear whether the two LG12 QTL regions detected in EL and WL fishes are actually the same or not, and it is hard to judge how different their genetic architectures are because our QTL analyses likely did not have power to detect loci of small effects. Nevertheless, genomic heritabilities for SL and BH (h^2 = 0.21–0.26) were very similar to the summed PVEs of individual QTL affecting these traits (0.11–0.27), suggesting an oligogenic basis of body size variation. This inference is supported by biometric estimates which have yielded very similar heritabilities within (h^2 = 0.13–0.18; Shimada et al., 2011) and among (h^2 = 0.07–0.25; Fraimout et al., 2022) population crosses in nine-spined sticklebacks.

We confirmed findings (Natri et al., 2019) that the ZW system inherited from *P. sinensis* controlled phenotypic sex of the hybrids between *P. sinensis* and *P. pungitius* and narrowed down this sex determination region. So far no sex determination gene has been identified in any *Pungitius* sticklebacks (Jeffries et al., 2022). Our study mapped sex-associated QTL to six genes, among which the Ubiquitin carboxyl-terminal hydrolase 7 (*Usp7*) has been found to regulate sex chromosome development and interact with the sex determination region in mice (Dong et al., 2021; Luo et al., 2015). Therefore, *Usp7* might also play some role in the sex determination of *P. sinensis*.

Among the genes that have been previously identified to have strong associations with the three-spined stickleback morphological development (summarized in Reid et al., 2021), only *Eda* on LG4 was included in our candidate gene list for the lateral plate number. Furthermore, we identified *Bmp2k* on LG13 as a candidate gene that impacts plate number variation in the nine-spined stickleback, and *Bmp7* on LG17 as a gene that potentially influences both plate number and plate width (although not plate area or height). Similarly, a recent study in the three-spined stickleback also found that the BMP pathway is a strong candidate mediating the effect of *Eda* on the development of lateral plates (Rodríguez-Ramírez et al., 2023). However, as all of the QTL regions in our study included tens to hundreds of genes, little confidence can be assigned to the identified candidate genes. Further narrowing of the QTL regions would require breeding individuals beyond F_2 generation, or adopting genome-wide association approaches with larger sample sizes than what was available for this study.

Marine nine-spined sticklebacks exhibit lower levels of gene flow and higher levels of genetic drift compared to three-spined sticklebacks (DeFaveri et al., 2012), which might have limited nine-spined sticklebacks more than three-spined sticklebacks in reaching their phenotypic optima when colonizing

freshwater habitats (Fang et al., 2021). For example, the previous study of three freshwater (pond) populations of EL nine-spined sticklebacks found that pelvic reduction was only complete in one population where it was controlled by a single large-effect locus (*pitx*1), whereas the other two populations only showed some level of pelvic reduction possibly controlled by alternative medium- or small-effect alleles at other QTL regions (Kemppainen et al., 2021). Similarly, the reduction of lateral plate numbers in both EL (Yang et al., 2016) and WL (this study) nine-spined sticklebacks is controlled by multiple medium- to small-effect loci that appear to be different from the large-effect *Eda* gene in three-spined sticklebacks. Accordingly, empirical evidence suggests that the hypothesis of parallel evolution in the repeatable phenotypic changes of freshwater *Pungitius* sticklebacks can be rejected, but indicates non-parallel and possibly redundant genetic architectures leading to similar phenotypic changes. Such redundancy is likely crucial for the evolutionary potential of species and populations facing rapid environmental changes, especially in fragmented habitats subject to increased genetic differentiation and bottlenecks. For the species with fragmented small populations, redundant genetic architectures increase the likelihood that at least some populations can adapt to some novel environmental pressures, but it is difficult to achieve adaptation in all traits within one population, and the long-term species survival probability will still depend on the spread of adaptive alleles across populations via gene flow.

Conclusions and outlook

In conclusion, our results add to the growing evidence (Fang et al., 2020; Kemppainen et al., 2021; Shapiro et al., 2009; Shikano et al., 2013; Yang et al., 2016) that the repeatability of evolutionary transitions in response to similar selection pressures in *Pungitius* sticklebacks appears to be often underlain by different genetic architectures of moderate- to small-effect loci. This differs from the situation in the closely related three-spined stickleback which tends to utilize the same major-effect loci to achieve similar phenotypic changes in independent colonizations of freshwater habitats. However, even in the case of the three-spined stickleback, growing evidence suggests that genetic parallelism in adaptation to freshwater is not as prevalent as early studies conducted in the Eastern Pacific region suggested: a greatly reduced degree of genetic parallelism has been found in the Atlantic basin likely due to variation lost during colonizations as well as reduced gene flow among these populations (Dahms et al., 2022; DeFaveri et al., 2011; Fang et al., 2020). The same also applies to stream-lake populations of three-spined sticklebacks experiencing reduced gene flow (Conte et al., 2012, 2015; Stuart et al., 2017; reviewed in Kemppainen et al., 2021). We suggest that further focus on genetic underpinnings of phenotypic variation in the morphologically and genetically diverse stickleback genus *Pungitius* (Guo et al., 2019) can provide a useful framework to quantify how the likelihood of genetic parallelism underlying similar phenotypic changes decreases with increasing evolutionary distance between taxa (Conte et al., 2012; Elmer & Meyer, 2011) and also inform us about variation in species' responses to changing environments (Bay et al., 2017).

Supplementary material

Supplementary material is available at *Journal of Evolutionary Biology* online.

Data availability

The raw RADseq data are available on NCBI BioProject PRJNA1124245. The raw digital photographs used for phenotypic measurements and the input data for R/qtl2 analyses are available in the Dryad repository (doi: 10.5061/dryad.tmpg4f54x; temporary link https://datadryad.org/stash/share/DCiegNimIbBDpojOBRy-JlktgZ--XQNZaX7laEBdlCE). Sample information and the raw phenotypes are available in the supplementary information. The R codes for analyses in this study are available on Github (https://github.com/xuelingyi/QTL_plate; DOI: 10.5281/zenodo.1155930).

Author contributions

Xueling Yi (Conceptualization [equal], Data curation [equal], Formal analysis [equal], Investigation [equal], Methodology [equal], Software [equal], Validation [equal], Visualization [lead], Writing—original draft [equal], Writing—review & editing [equal]), Petri Kemppainen (Data curation [equal], Formal analysis [equal], Methodology [equal], Validation [equal], Visualization [equal], Writing—original draft [equal], Writing—review & editing [equal]), Kerry Reid (Conceptualization [equal], Investigation [equal], Project administration [equal], Supervision [equal], Validation [equal], Writing—original draft [equal], Writing—review & editing [equal]), Ying Chen (Formal analysis [supporting], Investigation [supporting], Methodology [equal], Software [equal], Writing—review & editing [equal]), Pasi Rastas (Data curation [equal], Formal analysis [supporting], Methodology [equal], Software [equal]), Antoine Fraimout (Data curation [equal], Formal analysis [supporting], Methodology [equal], Software [equal], Validation [equal], Writing—review & editing [equal]), and Juha Merilä (Conceptualization [equal], Data curation [equal], Funding acquisition [equal], Investigation [equal], Project administration [equal], Resources [equal], Supervision [equal], Validation [equal], Writing—original draft [equal], Writing—review & editing [equal])

Funding

This study was supported by grants from Academy of Finland (250435, 263722, and 265211 to J.M.) and a grant from the Helsinki Life Sciences Institute (HiLIFE). Open access funded by Helsinki University Library.

Acknowledgments

We thank Heini Natri and Takahito Shikano for access to materials underlying this study, as well as all people who helped in obtaining the original samples (Akira Goto, Takefumi Kitamura, and Joost Rayemakers) and in fish breeding (Yukinori Shimada). Thanks are also due to Kirsi Kähkönen for help with DNA extractions. We gratefully acknowledge the computing resource support from CSC—the Finnish IT Center for Science Ltd administered by the Ministry of Education and Culture, Finland.

Conflicts of interest

None declared.

References

Albert, A. Y., Sawaya, S., Vines, T. H., … Schluter, D. (2008). The genetics of adaptive shape shift in stickleback: Pleiotropy and effect size. *Evolution*, *62*(1), 76–85.

Bailey, S. F., Blanquart, F., Bataillon, T., & Kassen, R. (2017). What drives parallel evolution? *Bioessays*, *39*(1), 1–9. https://doi.org/10.1002/bies.201600176

Baird, N. A., Etter, P. D., Atwood, T. S., … Johnson, E. A. (2008). Rapid SNP discovery and genetic mapping using sequenced RAD markers. *PLoS One*, *3*(10), e3376.

Banarescu, P. M., & Paepke, H. J. (2001). *The freshwater fishes of Europe* (Vol. *5/III)*. AULA.

Bay, R. A., Rose, N., Barrett, R., … Ralph, P. (2017). Predicting responses to contemporary environmental change using evolutionary response architectures. *The American Naturalist*, *189*(5), 463–473. https://doi.org/10.1086/691233

Bernatchez, L., Renaut, S., Whiteley, A. R., … St-Cyr, J. (2010). On the origin of species: Insights from the ecological genomics of lake whitefish. *Philosophical Transactions of the Royal Society of London, Series B: Biological Sciences*, *365*(1547), 1783–1800. https://doi.org/10.1098/rstb.2009.0274

Berner, D., Moser, D., Roesti, M., … Salzburger, W. (2014). Genetic architecture of skeletal evolution in European lake and stream stickleback. *Evolution*, *68*(6), 1792–1805. https://doi.org/10.1111/evo.12390

Bolnick, D. I., Barrett, R. D. H., Oke, K. B., … Stuart, Y. E. (2018). (Non)Parallel evolution. *Annual Review of Ecology, Evolution, and Systematics*, *49*, 303–333. https://doi.org/10.1146/annurev-ecolsys-110617

Broman, K. W., Gatti, D. M., Simecek, P., … Churchill, G. A. (2019). R/qtl2: Software for mapping quantitative trait loci with high-dimensional data and multiparent populations. *Genetics*, *211*(2), 495–502. https://doi.org/10.1534/GENETICS.118.301595

Broman, K. W., & Sen, Ś. (2009). *A guide to QTL mapping with R/qtl* (Vol. *46*). Springer.

Chan, Y. F., Marks, M. E., Jones, F. C., … Kingsley, D. M. (2010). Adaptive evolution of pelvic reduction in sticklebacks by recurrent deletion of a Pitx1 enhancer. *Science*, *327*(5963), 302–305. https://doi.org/10.1126/science.1182213

Colosimo, P. F., Hosemann, K. E., Balabhadra, S., … Kingsley, D. M. (2005). Widespread parallel evolution in sticklebacks by repeated fixation of ectodysplasin alleles. *Science*, *307*(5717), 1928–1933. https://doi.org/10.1126/SCIENCE.1107239

Colosimo, P. F., Peichel, C. L., Nereng, K., … Kingsley, D. M. (2004). The genetic architecture of parallel armor plate reduction in threespine sticklebacks. *PLoS Biology*, *2*(5), E109–e109. https://doi.org/10.1371/journal.pbio.0020109

Conte, G. L., Arnegard, M. E., Best, J., … Peichel, C. L. (2015). Extent of QTL reuse during repeated phenotypic divergence of sympatric threespine stickleback. *Genetics*, *201*(3), 1189–1200. https://doi.org/10.1534/genetics.115.182550

Conte, G. L., Arnegard, M. E., Peichel, C. L., & Schluter, D. (2012). The probability of genetic parallelism and convergence in natural populations. *Proceedings Biological Sciences*, *279*(1749), 5039–5047. https://doi.org/10.1098/rspb.2012.2146

Coyle, S. M., Huntingford, F. A., & Peichel, C. L. (2007). Parallel evolution of *Pitx1* underlies pelvic reduction in Scottish threespine stickleback (*Gasterosteus aculeatus*). *The Journal of Heredity*, *98*(6), 581–586. https://doi.org/10.1093/jhered/esm066

Cresko, W. A., Amores, A., Wilson, C., … Postlethwait, J. H. (2004). Parallel genetic basis for repeated evolution of armor loss in Alaskan threespine stickleback populations. *Proceedings of the National Academy of Sciences*, *101*(16), 6050–6055.

Dahms, C., Kemppainen, P., Zanella, L. N., … Momigliano, P. (2022). Cast away in the Adriatic: Low degree of parallel genetic differentiation in three-spined sticklebacks. *Molecular Ecology*, *31*(4), 1234–1253. https://doi.org/10.1111/mec.16295

Danecek, P., Bonfield, J. K., Liddle, J., … Li, H. (2021). Twelve years of SAMtools and BCFtools. *GigaScience*, *10*(2), giab008. https://doi.org/10.1093/gigascience/giab008

DeFaveri, J., Jonsson, P. R., & Merilä, J. (2013). Heterogeneous genomic differentiation in marine threespine sticklebacks: Adaptation along an environmental gradient. *Evolution*, *67*(9), 2530–2546. https://doi.org/10.1111/evo.12097

DeFaveri, J., Shikano, T., Ghani, N. I. A., & Merilä, J. (2012). Contrasting population structures in two sympatric fishes in the Baltic Sea basin. *Marine Biology*, *159*(8), 1659–1672. https://doi.org/10.1007/s00227-012-1951-4

DeFaveri, J., Shikano, T., Shimada, Y., … Merilä, J. (2011). Global analysis of genes involved in freshwater adaptation in threespine sticklebacks (*Gasterosteus aculeatus*). *Evolution*, *65*(6), 1800–1807. https://doi.org/10.1111/j.1558-5646.2011.01247.x

Dong, X., Xu, X., Yang, C., … Wang, J.. (2021). USP7 regulates the proliferation and differentiation of ATDC5 cells through the Sox9-PTHrP-PTH1R axis. *Bone*, *143*, 115714. https://doi.org/10.1016/j.bone.2020.115714

Elmer, K. R., Kusche, H., Lehtonen, T. K., & Meyer, A. (2010). Local variation and parallel evolution: Morphological and genetic diversity across a species complex of neotropical crater lake cichlid fishes. *Philosophical Transactions of the Royal Society of London, Series B: Biological Sciences*, *365*(1547), 1763–1782. https://doi.org/10.1098/rstb.2009.0271

Elmer, K. R., & Meyer, A. (2011). Adaptation in the age of ecological genomics: Insights from parallelism and convergence. *Trends in Ecology & Evolution*, *26*(6), 298–306. https://doi.org/10.1016/j.tree.2011.02.008

Erickson, P. A., Glazer, A. M., Killingbeck, E. E., … Miller, C. T. (2016). Partially repeatable genetic basis of benthic adaptation in threespine sticklebacks. *Evolution*, *70*(4), 887–902. https://doi.org/10.1111/evo.12897

Fang, B., Kemppainen, P., Momigliano, P., … Merilä, J. (2020). On the causes of geographically heterogeneous parallel evolution in sticklebacks. *Nature Ecology & Evolution 2020*, *4*(8), 1105–1115. https://doi.org/10.1038/s41559-020-1222-6

Fang, B., Kemppainen, P., Momigliano, P., & Merilä, J. (2021). Population structure limits parallel evolution in sticklebacks. *Molecular Biology and Evolution*, *38*(10), 4205–4221. https://doi.org/10.1093/molbev/msab144

Feng, X., Merilä, J., & Löytynoja, A. (2022). Complex population history affects admixture analyses in nine-spined sticklebacks. *Molecular Ecology*, *31*(20), 5386–5401. https://doi.org/10.1111/mec.16651

Fraimout, A., Li, Z., Sillanpää, M. J., & Merilä, J. (2022). Age-dependent genetic architecture across ontogeny of body size in sticklebacks. *Proceedings of the Royal Society B: Biological Sciences*, *289*(1975), 20220352. https://doi.org/10.1098/rspb.2022.0352

Glazer, A. M., Killingbeck, E. E., Mitros, T., … Miller, C. T. (2015). Genome assembly improvement and mapping convergently evolved skeletal traits in sticklebacks with genotyping-by-sequencing. *G3 (Bethesda, Md.)*, *5*(7), 1463–1472. https://doi.org/10.1534/g3.115.017905

Guo, B., Fang, B., Shikano, T., … Merilä, J. (2019). A phylogenomic perspective on diversity, hybridization and evolutionary affinities in the stickleback genus Pungitius. *Molecular Ecology*, *28*(17), 4046–4064. https://doi.org/10.1111/mec.15204

Indjeian, V. B., Kingman, G. A., Jones, F. C., … Kingsley, D. M. (2016). Evolving new skeletal traits by cis-regulatory changes in bone morphogenetic proteins. *Cell*, *164*(1-2), 45–56. https://doi.org/10.1016/j.cell.2015.12.007

Jeffries, D. L., Mee, J. A., & Peichel, C. L. (2022). Identification of a candidate sex determination gene in *Culaea inconstans* suggests convergent recruitment of an *Amh* duplicate in two lineages of stickleback. *Journal of Evolutionary Biology*, *35*(12), 1683–1695. https://doi.org/10.1111/jeb.14034

Johannesson, K. (2001). Parallel speciation: A key to sympatric divergence. *Trends in Ecology & Evolution*, *16*(3), 148–153. https://doi.org/10.1016/s0169-5347(00)02078-4

Jones, F. C., Grabherr, M. G., Chan, Y. F., … Kingsley, D. M.; Broad Institute Genome Sequencing Platform & Whole Genome Assembly Team (2012). The genomic basis of adaptive evolution in

threespine sticklebacks. *Nature*, *484*(7392), 55–61. https://doi.org/10.1038/nature10944

Jovelin, R., He, X., Amores, A., … Postlethwait, J. H. (2007). Duplication and divergence of fgf8 functions in teleost development and evolution. *Journal of Experimental Zoology. Part B. Molecular and Developmental Evolution*, *308B*(6), 730–743. https://doi.org/10.1002/jez.b.21193

Kemppainen, P., Li, Z., Rastas, P., … Merilä, J. (2021). Genetic population structure constrains local adaptation in sticklebacks. *Molecular Ecology*, *30*(9), 1946–1961. https://doi.org/10.1111/mec.15808

Kivikoski, M., Rastas, P., Löytynoja, A., & Merilä, J. (2021). Automated improvement of stickleback reference genome assemblies with Lep-Anchor software. *Molecular Ecology Resources*, *21*(6), 2166–2176. https://doi.org/10.1111/1755-0998.13404

Kivikoski, M., Rastas, P., Löytynoja, A., & Merilä, J. (2023). Predicting recombination frequency from map distance. *Heredity*, *130*(3), 114–121. https://doi.org/10.1038/s41437-022-00585-3

Laine, V. N., Shikano, T., Herczeg, G., … Merilä, J. (2013). Quantitative trait loci for growth and body size in the nine-spined stickleback *Pungitius pungitius* L. *Molecular Ecology*, *22*(23), 5861–5876. https://doi.org/10.1111/mec.12526

Lang, D., Powell, S. K., Plummer, R. S., … Ruggeri, B. A. (2007). PAX genes: Roles in development, pathophysiology, and cancer. *Biochemical Pharmacology*, *73*(1), 1–14. https://doi.org/10.1016/j.bcp.2006.06.024

Laurentino, T. G., Boileau, N., Ronco, F., & Berner, D. (2022). The ectodysplasin-A receptor is a candidate gene for lateral plate number variation in stickleback fish. *G3 (Bethesda, Md.)*, *12*(6), jkac077. https://doi.org/10.1093/g3journal/jkac077

Lee, K. M., & Coop, G. (2017). Distinguishing among modes of convergent adaptation using population genomic data. *Genetics*, *207*(4), 1591–1619. https://doi.org/10.1534/genetics.117.300417

Leinonen, T., McCairns, R. J. S., Herczeg, G., & Merilä, J. (2012). Multiple evolutionary pathways to decreased lateral plate coverage in freshwater threespine sticklebacks. *Evolution*, *66*(12), 3866–3875. https://doi.org/10.1111/j.1558-5646.2012.01724.x

Li, H. (2011). A statistical framework for SNP calling, mutation discovery, association mapping and population genetical parameter estimation from sequencing data. *Bioinformatics*, *27*(21), 2987–2993. https://doi.org/10.1093/bioinformatics/btr509

Li, H., & Durbin, R. (2009). Fast and accurate short read alignment with Burrows–Wheeler transform. *Bioinformatics*, *25*(14), 1754–1760. https://doi.org/10.1093/bioinformatics/btp324

Li, X., & Cao, X. (2006). BMP signaling and skeletogenesis. *Annals of the New York Academy of Sciences*, *1068*(1), 26–40. https://doi.org/10.1196/annals.1346.006

Li, Z., Guo, B., Yang, J., … Merilä, J. (2017). Deciphering the genomic architecture of the stickleback brain with a novel multilocus gene-mapping approach. *Molecular Ecology*, *26*(6), 1557–1575. https://doi.org/10.1111/mec.14005

Li, Z., Kemppainen, P., Rastas, P., & Merilä, J. (2018). Linkage disequilibrium clustering-based approach for association mapping with tightly linked genomewide data. *Molecular Ecology Resources*, *18*(4), 809–824. https://doi.org/10.1111/1755-0998.12893

Liu, J., Shikano, T., Leinonen, T., … Merilä, J. (2014). Identification of major and minor QTL for ecologically important morphological traits in three-spined sticklebacks (*Gasterosteus aculeatus*). *G3 (Bethesda, Md.)*, *4*(4), 595–604. https://doi.org/10.1534/g3.114.010389

Loehr, J., Leinonen, T., Herczeg, G., … Merilä, J. (2012). Heritability of asymmetry and lateral plate number in the threespine stickleback. *PLoS One*, *7*(7), e39843–e39843. https://doi.org/10.1371/journal.pone.0039843

Lucek, K., Haesler, M. P., & Sivasundar, A. (2012). When phenotypes do not match genotypes—unexpected phenotypic diversity and potential environmental constraints in Icelandic stickleback. *The Journal of Heredity*, *103*(4), 579–584. https://doi.org/10.1093/jhered/ess021

Luo, M., Zhou, J., Leu, N. A., … Wang, P. J. (2015). Polycomb protein SCML2 associates with USP7 and counteracts histone H2A ubiquitination in the XY chromatin during male meiosis. *PLoS Genetics*, *11*(1), e1004954. https://doi.org/10.1371/journal.pgen.1004954

MacPherson, A., & Nuismer, S. L. (2017). The probability of parallel genetic evolution from standing genetic variation. *Journal of Evolutionary Biology*, *30*(2), 326–337. https://doi.org/10.1111/jeb.13006

Marchinko, K. B., & Schluter, D. (2007). Parallel evolution by correlated response: Lateral plate reduction in threespine stickleback. *Evolution*, *61*(5), 1084–1090. https://doi.org/10.1111/j.1558-5646.2007.00103.x

Martin, A., & Orgogozo, V. (2013). The loci of repeated evolution: A catalog of genetic hotspots of phenotypic variation. *Evolution*, *67*(5), 1235–1250. https://doi.org/10.1111/evo.12081

Merilä, J. (2013). Nine-spined stickleback (*Pungitius pungitius*): An emerging model for evolutionary biology research. *Annals of the New York Academy of Sciences*, *1289*(1), 18–35. https://doi.org/10.1111/nyas.12089

Merilä, J. (2014). Lakes and ponds as model systems to study parallel evolution. *Journal of Limnology*, *73*(s1), 33–45. https://doi.org/10.4081/JLIMNOL.2014.805

Miller, C. T., Glazer, A. M., Summers, B. R., … Kingsley, D. M. (2014). Modular skeletal evolution in sticklebacks is controlled by additive and clustered quantitative trait loci. *Genetics*, *197*(1), 405–420. https://doi.org/10.1534/genetics.114.162420

Miller, M. R., Dunham, J. P., Amores, A., … Johnson, E. A. (2007). Rapid and cost-effective polymorphism identification and genotyping using restriction site associated DNA (RAD) markers. *Genome Research*, *17*(2), 240–248. https://doi.org/10.1101/gr.5681207

Natri, H. M., Merilä, J., & Shikano, T. (2019). The evolution of sex determination associated with a chromosomal inversion. *Nature Communications*, *10*(1), 1–13. https://doi.org/10.1038/s41467-018-08014-y

O'Brown, N. M., Summers, B. R., Jones, F. C., … Kingsley, D. M. (2015). (2015). A recurrent regulatory change underlying altered expression and Wnt response of the stickleback armor plates gene EDA. *eLife*, *4*(4), e05290. https://doi.org/10.7554/eLife.05290

Peichel, C. L., & Marques, D. A. (2017). The genetic and molecular architecture of phenotypic diversity in sticklebacks. *Philosophical Transactions of the Royal Society B: Biological Sciences*, *372*(1713), 20150486. https://doi.org/10.1098/rstb.2015.0486

Peichel, C. L., Nereng, K. S., Ohgi, K. A., … Kingsley, D. M. (2001). The genetic architecture of divergence between threespine stickleback species. *Nature*, *414*(6866), 901–905.

Poore, H. A., Stuart, Y. E., Rennison, D. J., … Peichel, C. L. (2023). Repeated genetic divergence plays a minor role in repeated phenotypic divergence of lake-stream stickleback. *Evolution*, *77*(1), 110–122. https://doi.org/10.1093/evolut/qpac025

R Core Team. (2022). R: A language and environment for statistical computing. R Foundation for Statistical Computing. https://www.R-project.org/

Ralph, P. L., & Coop, G. (2015). The role of standing variation in geographic convergent adaptation. *The American Naturalist*, *186*(Suppl 1), S5–23. https://doi.org/10.1086/682948

Rastas, P. (2017). Lep-MAP3: Robust linkage mapping even for low-coverage whole genome sequencing data. *Bioinformatics*, *33*(23), 3726–3732. https://doi.org/10.1093/bioinformatics/btx494

Rastas, P. (2020). Lep-Anchor: Automated construction of linkage map anchored haploid genomes. *Bioinformatics*, *36*(8), 2359–2364. https://doi.org/10.1093/bioinformatics/btz978

Reid, K., Bell, M. A., & Veeramah, K. R. (2021). Threespine stickleback: A model system for evolutionary genomics. *Annual Review of Genomics and Human Genetics*, *22*(1), 357–383. https://doi.org/10.1146/annurev-genom-111720-081402

Rennison, D. J., & Peichel, C. L. (2022). Pleiotropy facilitates parallel adaptation in sticklebacks. *Molecular Ecology*, *31*(5), 1476–1486. https://doi.org/10.1111/mec.16335

Roberts Kingman, G. A., Vyas, D. N., Jones, F. C., … Veeramah, K. R. (2021). Predicting future from past: The genomic basis of recurrent and rapid stickleback evolution. *Science Advances*, *7*(25), eabg5285.

Rodríguez-Ramírez, C. E., Hiltbrunner, M., Saladin, V., … Peichel, C. L. (2023). Molecular mechanisms of *Eda*-mediated adaptation to freshwater in threespine stickleback. *Molecular Ecology*, 1–19. https://doi.org/10.1111/mec.16989

Roesti, M. (2018). Varied genomic responses to maladaptive gene flow and their evidence. *Genes*, *9*(6), 298. https://doi.org/10.3390/genes9060298

Schlötterer, C. (2023). How predictable is adaptation from standing genetic variation? Experimental evolution in *Drosophila* highlights the central role of redundancy and linkage disequilibrium. *Philosophical Transactions of the Royal Society B: Biological Sciences*, *378*(1877), 0046. https://doi.org/10.1098/rstb.2022.0046

Schluter, D., Clifford, E. A., Nemethy, M., & McKinnon, J. S. (2004). Parallel evolution and inheritance of quantitative traits. *The American Naturalist*, *163*(6), 809–822. https://doi.org/10.1086/383621

Schluter, D., Marchinko, K. B., Arnegard, M. E., … Kingsley, D. M. (2021). Fitness maps to a large-effect locus in introduced stickleback populations. *Proceedings of the National Academy of Sciences of the United States of America*, *118*(3), e1914889118. https://doi.org/10.1073/pnas.1914889118

Shapiro, M. D., Summers, B. R., Balabhadra, S., … Kingsley, D. M. (2009). The Genetic architecture of skeletal convergence and sex determination in ninespine sticklebacks. *Current Biology: CB*, *19*(13), 1140–1145. https://doi.org/10.1016/j.cub.2009.05.029

Shawi, M., & Serluca, F. C. (2008). Identification of a BMP7 homolog in zebrafish expressed in developing organ systems. *Gene Expression Patterns: GEP*, *8*(6), 369–375. https://doi.org/10.1016/j.gep.2008.05.004

Shikano, T., Laine, V. N., Herczeg, G., … Merilä, J. (2013). Genetic architecture of parallel pelvic reduction in ninespine sticklebacks. *G3 (Bethesda, Md.)*, *3*(10), 1833–1842. https://doi.org/10.1534/g3.113.007237

Shikano, T., Shimada, Y., Herczeg, G., & Merilä, J. (2010). History vs. habitat type: Explaining the genetic structure of European nine-spined stickleback (*Pungitius pungitius*) populations. *Molecular Ecology*, *19*(6), 1147–1161. https://doi.org/10.1111/j.1365-294X.2010.04553.x

Shimada, Y., Shikano, T., Kuparinen, A., … Merilä, J. (2011). Quantitative genetics of body size and timing of maturation in two ninespined stickleback (*Pungitius pungitius*) populations. *PLoS One*, *6*(12), e28859. https://doi.org/10.1371/journal.pone.0028859

Smith, S. R., Amish, S. J., Bernatchez, L., … Scribner, K. T. (2020). Mapping of adaptive traits enabled by a high-density linkage map for lake trout. *G3 Genes|Genomes|Genetics*, *10*(6), g3.401184.2020–g3.401184.1947. https://doi.org/10.1534/g3.120.401184

Stewart, J. R., & Thompson, M. B. (2009). Parallel evolution of placentation in Australian scincid lizards. *Journal of Experimental Zoology. Part B. Molecular and Developmental Evolution*, *312B*(6), 590–602. https://doi.org/10.1002/jez.b.21245

Stuart, Y. E., Veen, T., Weber, J. N., … Bolnick, D. I. (2017). Contrasting effects of environment and genetics generate a continuum of parallel evolution. *Nature Ecology & Evolution*, *1*(6), Article 6. https://doi.org/10.1038/s41559-017-0158

Sunnucks, P., & Hales, D. F. (1996). Numerous transposed sequences of mitochondrial cytochrome oxidase I-II in aphids of the genus *Sitobion* (Hemiptera: Aphididae). *Molecular Biology and Evolution*, *13*(3), 510–524. https://doi.org/10.1093/oxfordjournals.molbev.a025612

Takahashi, H., Takata, K., & Goto, A. (2001). Phylogeography of lateral plate dimorphism in the freshwater type of ninespine sticklebacks, genus *Pungitius*. *Ichthyological Research*, *48*(2), 143–154. https://doi.org/10.1007/s10228-001-8129-2

Teacher, A. G. F., Shikano, T., Karjalainen, M. E., & Merilä, J. (2011). Phylogeography and genetic structuring of European nine-spined sticklebacks (*Pungitius pungitius*)—Mitochondrial DNA evidence. *PLoS One*, *6*(5), e19476–e19476. https://doi.org/10.1371/journal.pone.0019476

Thompson, K. A., Osmond, M. M., & Schluter, D. (2019). Parallel genetic evolution and speciation from standing variation. *Evolution Letters*, *3*(2), 129–141. https://doi.org/10.1002/evl3.106

Trokovic, N., Herczeg, G., Scott McCairns, R. J., … Merilä, J. (2011). Intraspecific divergence in the lateral line system in the nine-spined stickleback (*Pungitius pungitius*). *Journal of Evolutionary Biology*, *24*(7), 1546–1558. https://doi.org/10.1111/j.1420-9101.2011.02286.x

Varadharajan, S., Rastas, P., Löytynoja, A., … Merilä, J. (2019). A high-quality assembly of the nine-spined stickleback (*Pungitius pungitius*) genome. *Genome Biology and Evolution*, *11*(11), 3291–3308. https://doi.org/10.1093/gbe/evz240

Wang, C., Shikano, T., Persat, H., & Merilä, J. (2015). Mitochondrial phylogeography and cryptic divergence in the stickleback genus *Pungitius*. *Journal of Biogeography*, *42*(12), 2334–2348. https://doi.org/10.1111/jbi.12591

Wang, M., Zhang, T., Zhang, X., … Huang, Z. (2020). BMP2K dysregulation promotes abnormal megakaryopoiesis in acute megakaryoblastic leukemia. *Cell & Bioscience*, *10*(1), 57. https://doi.org/10.1186/s13578-020-00418-y

Xie, K. T., Wang, G., Thompson, A. C., … Kingsley, D. M. (2019). DNA fragility in the parallel evolution of pelvic reduction in stickleback fish. *Science*, *363*(6422), 81–84.

Yamasaki, Y. Y., Mori, S., Kokita, T., & Kitano, J. (2019). Armour plate diversity in Japanese freshwater threespine stickleback (Gasterosteus aculeatus). *Evolutionary Ecology Research*, *20*(1), 51–67.

Yang, J., Guo, B., Shikano, T., … Merilä, J. (2016). Quantitative trait locus analysis of body shape divergence in nine-spined sticklebacks based on high-density SNP-panel. *Scientific Reports*, *6*(1), 26632. https://doi.org/10.1038/srep26632